Nitrogen in germanium: Identification of the pair defect

F. Berg Rasmussen
Institute of Physics and Astronomy, University of Aarhus, DK-8000 Århus C, Denmark

R. Jones
Department of Physics, University of Exeter, EX44QL Exeter, United Kingdom

S. Öberg
Department of Mathematics, University of Luleå, S-95187 Luleå, Sweden

(Received 4 March 1994)

Several nitrogen-related centers have been introduced by ion implantation of nitrogen into germanium and studied by infrared-absorption spectroscopy. Two local vibrational modes at 825.3 and 658.6 cm^{-1} were especially prominent. Measurements on annealed samples implanted with either pure ^{14}N or ^{15}N, or implanted with both isotopes showed these modes to arise from a nitrogen pair defect analogous to one previously suggested to occur in silicon. Based on this and *ab initio* pseudopotential cluster theory, a model of the pair is proposed which is consistent with the observed infrared absorption. This model is similar to that of the nitrogen pair in silicon and offers an explanation of the low donor efficiency of nitrogen in germanium. Several other nitrogen-related local vibrational modes are also observed in the implanted material.

I. INTRODUCTION

The electronic and optical properties of semiconducting materials are often determined by the presence of chemical impurities and the study of these defects in group-IV and III-V semiconductors has a long and distinguished history. The elucidation of the properties of these defects is of technological importance and yet still continues to pose problems.

Nitrogen (N) is an interesting impurity in silicon (Si) and germanium (Ge) as it shows anomalous electrical behavior. Contrary to the other group-V members such as phosphorus or arsenic, N only shows weak donor activity in crystalline Si (Ref. 1) and Ge.[2] This is partly related to its low solubility,[3] for in the high concentrations present in the hydrogenated amorphous materials (*a*-Si:H, *a*-Ge:H), N readily acts as a donor.[4,5] However, in Si the large majority of the N impurities form pairs in implanted as well as in grown material.[6] The structure of this pair has only recently been established[7] and it consists of two neighboring ⟨100⟩-oriented Si-N split interstitials, arranged in an antiparallel configuration and with the four bonds forming a square lying on {011} (Fig. 1). This major defect is electrically inert and any electrical activity arising from N must be due to other defects.[7]

Stein[8] has measured the infrared absorption of N ion implanted into Ge after laser annealing. Four local vibrational modes (LVM) were detected at 825, 660, 590, and 577 cm^{-1} in ^{14}N-implanted samples and these shifted to 801, 641, 573, and 559 cm^{-1}, respectively, in the case of ^{15}N. These are analogous to the LVM's at 967, 771, 691, and 658 cm^{-1} (80 K) observed in N-implanted Si.[8]

Substitutional N (N_s) in the neutral charge state gives rise to the electron paramagnetic resonance (EPR) spectrum SL5 (Ref. 9) in Si and the 658-cm^{-1} LVM was correlated to this defect via production and annealing characteristics by Stein.[10] Although a corresponding EPR spectrum has not been observed in N-implanted Ge, Stein[8] assigned the 577-cm^{-1} mode to a N_s. The 691-cm^{-1} N mode in Si has been suggested to be a Si-N stretch mode of a N interstitial (N_i) and in analogy with this, Stein[8] ascribed the 590-cm^{-1} mode in Ge to a Ge-N stretch of a N_i. The two modes at 660 and 825 cm^{-1}

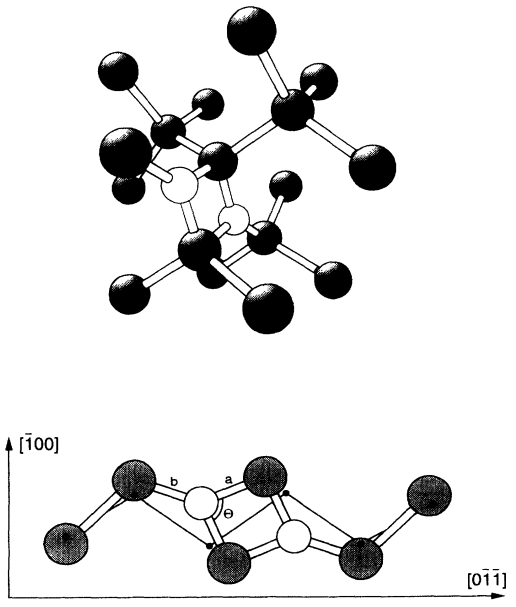

FIG. 1. The antiparallel model of the N pair defect (Ref. 7) shown in perspective and in the {110} mirror plane. The small points mark the substitutional (perfect lattice) sites. The upper part of the figure has been reproduced from Ref. 7.

were attributed to a N-pair defect but no direct evidence for pairing of the N atoms was given. Clearly further work is needed to understand the basic properties of N as an impurity in Ge and especially the structural and dynamical properties of the N defects giving rise to the two major modes at 825 and 660 cm^{-1} (^{14}N).

In this work we address this problem and it is shown that the two modes actually originate from a N-pair defect. We also confirm the assignments made by Stein for the 577- and 590-cm^{-1} modes. Moreover, we propose a consistent model for the pair defect. Our results are based on the measured infrared absorption and on *ab initio* theory. These methods combined with results deduced from channeling have been used earlier to infer the structures and local vibrational modes of the substitutional, interstitial, and pair N defects in Si.[7] Our model for the pair defects involves two ⟨100⟩ Ge-N split interstitials arranged in the antiparallel configuration shown in Fig. 1. The fact that the solubility of N in Si and Ge is so low, together with the tendency for N to pair in this way, explains the low efficiency for donor activity in these materials. In addition, we report on several other N-related LVM's in Ge.

II. EXPERIMENTAL DETAILS

The Ge samples used in this study were made of ⟨100⟩-oriented *p*-type high-purity material with a stated impurity concentration of less than 8×10^{9} cm^{-3}. The samples were cut into $5\times5\times2$-mm^3 sections whose square faces were polished for the optical studies. The samples were then implanted on both sides at room temperature with either ^{14}N, ^{15}N, or both isotopes. The implantations were done at energies of 70, 120, 180, 250, 350, 450, and 500 keV using a 600-keV electrostatic accelerator equipped with a universal ion source and a large magnet for mass separation. The samples were tilted 7° off the beam direction to avoid channeling effects and the beam was horizontally and vertically swept in order to ensure a homogenous lateral distribution over the sample. The implanted dose was determined from the current measured on the sample which was surrounded by a shield biased to −300 V to reduce the effect of secondary electrons. The uncertainty on the implanted dose is about 5%. The doses were chosen to obtain a nearly uniform profile of density 6.5×10^{19} cm^{-3} from 0.1 to 0.8 μm on each side. After implantation, isochronal 30-min annealing experiments were performed using a conventional flow oven and temperature steps of approximately 50 °C. After each anneal the samples were given a short etch in HF to remove surface oxides and then infrared absorption spectra were measured at 77 K using a Nicolet System 800 FTIR spectrometer equipped with an MCT detector and a Ge-KBr beam splitter. The number of scans was typically 200 and the apodized resolution was 3.8 cm^{-1}. From 400 °C and above, where the samples have recrystallized, spectra with a better resolution (1 cm^{-1}) were also measured in order to determine the positions and the widths of the modes with higher accuracy and to detect any fine structure due to the different Ge isotopes.

III. EXPERIMENTAL RESULTS

The infrared absorption of the ^{14}N-implanted sample after annealing at 402 °C is shown in Fig. 2(a). The two strong modes at 659 and 825 cm^{-1} observed in ^{14}N-implanted samples shift to 640 and 799 cm^{-1} with ^{15}N [Fig. 2(b)] These LVM's are identical to the "pair-modes" observed by Stein and they will be denoted as such in the following. In the sample containing equal amounts of ^{14}N and ^{15}N two intermediate modes at 654 and 810 cm^{-1} are also observed [Fig. 2(c)]. The intensity of these intermediate modes is close to twice that of the modes due to ^{14}N and ^{15}N. This is demonstrated in Fig. 2(d) where one-fourth of the pure ^{14}N and ^{15}N spectra has been subtracted from the mixed isotopic spectrum in Fig. 2(c). The two modes at 628 and 609 cm^{-1} seen in the mixed isotopic spectrum of Fig. 2(c) [and Fig. 2(d)] were only observed in this sample. They have annealing characteristics different from the other modes shown in Fig. 2 and they will not be discussed further.

When the material is annealed at higher temperatures, other modes appear as shown in Fig. 3. These modes begin to appear around 450 °C but disappear at 700 °C and

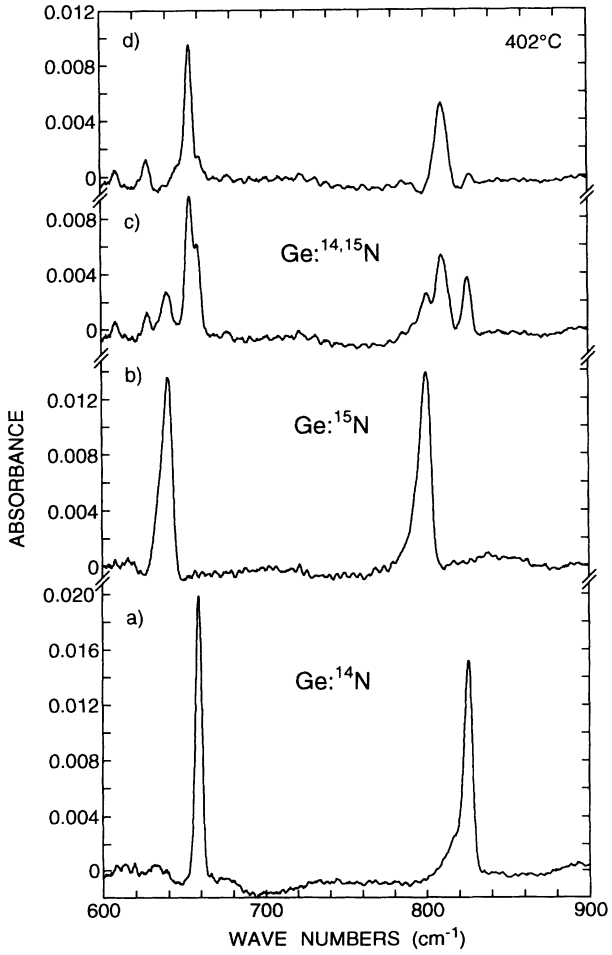

FIG. 2. Absorbance spectrum observed after annealing at 402 °C of samples implanted with ^{14}N (a), ^{15}N (b), or equal doses of both isotopes (c). (d) is discussed in the text.

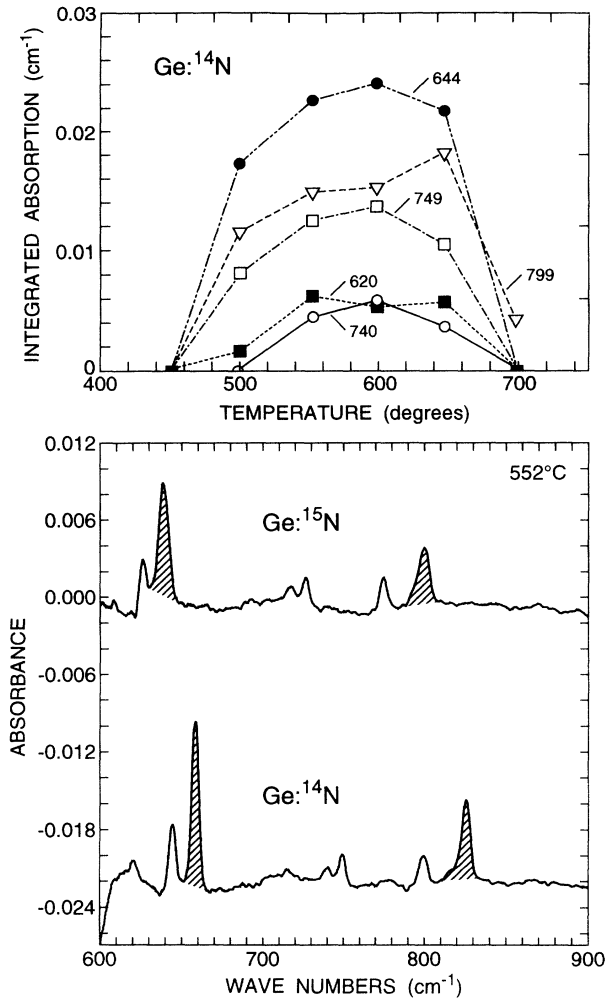

FIG. 3. Isochronal annealing curves of the other N-related local vibrational modes (^{14}N). Also shown is the absorbance after annealing at 552 °C of samples implanted with ^{14}N or ^{14}N; the pair modes also observed at 402 °C have been hatched. The Ge:^{14}N spectrum has been displaced vertically for clarity.

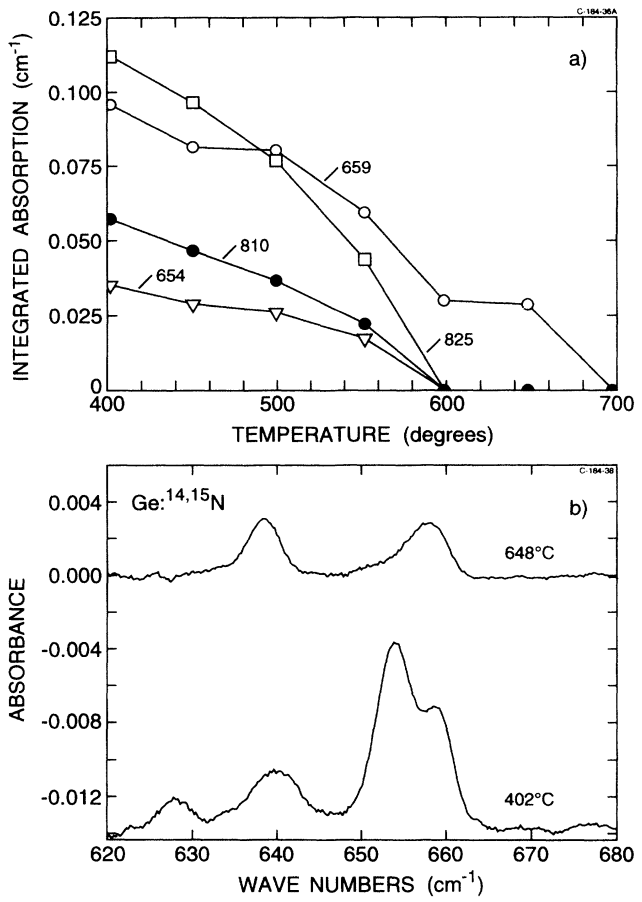

FIG. 4. Isochronal annealing curves of the pair modes at 825 and 659 cm^{-1} observed in the ^{14}N sample and of the intermediate modes at 810 and 654 cm^{-1} observed in the sample implanted with both ^{14}N and ^{15}N into overlapping profiles (a). Also shown is a section of the absorbance spectrum of the mixed isotopic sample after annealing at 402 and 648 °C (b). The 402 °C spectrum has been displaced vertically for clarity.

they show isotopic shifts with ^{15}N (see Fig. 3). In the mixed isotopic sample the other modes were only weakly detectable suggesting that the responsible defects contain many N atoms leading to broadened spectra in the mixed case. Our main concern here is the pair modes originally observed by Stein and their mixed isotopic analogues. All the other N-related modes have different annealing properties and hence they will not be discussed any further in this paper. The annealing properties of the new modes are shown in Fig. 3 and the line positions are listed in Table I.

Figure 4(a) shows the isochronal annealing behavior of the two pair modes at 659 and 825 cm^{-1} (^{14}N) as well as the annealing of the two intermediate modes at 654 and 810 cm^{-1} observed in the mixed isotopic sample. The 825-, 654-, and 810-cm^{-1} modes are clearly correlated whereas the 659-cm^{-1} mode drops at about the same rate as the other modes below 600 °C but exhibits a shoulder above 600 °C.

TABLE I. Positions in cm^{-1} of the other N-related local vibrational modes. See the text for an explanation of the *.

^{14}N	620	644	659*	740	749	799
^{15}N	608	626	637*	717	726	774

IV. INTERPRETATION OF EXPERIMENTAL RESULTS

The two LVM's at 659 and 825 cm^{-1} shown in Fig. 2(a) show isotopic shifts when ^{14}N is substituted by ^{15}N [Fig. 2(b)], consequently both modes are due to N-related defects. Moreover, both modes arise from defects involving a pair of N atoms as they both show an intermediate mode in the sample implanted with both ^{14}N and ^{15}N [Fig. 2(c)], and as the intensities are very nearly proportional to the expected concentration of pairs of the various isotopes [(Fig. 2(d)]. The existence of N-pair defects in Ge has hereby been established.

It is tempting to suggest that we are dealing with one type of N pair and hence that the pair modes actually arise from the same defect. That this is actually the case

is evidenced by the fact that the two intermediate modes at 654 and 810 cm^{-1} have the same annealing behavior as shown in Fig. 4(a). For consistency the annealing of the pair modes observed in the pure isotopic samples should be correlated to those of the intermediate pair modes. This is clearly the case for the high-frequency mode at 825 cm^{-1} (^{14}N) but not quite as obvious for the low-frequency mode at 659 cm^{-1} because of the observed shoulder above 600 °C [see Fig. 4(a)].

After annealing at 648 °C, where the 825-cm^{-1} mode has disappeared, a mode at 659 cm^{-1} is still observed in the ^{14}N-implanted sample and this mode shifts to 637 cm^{-1} with ^{15}N. In the mixed isotopic sample two modes of equal intensity at 637 and 659 cm^{-1} are observed after annealing at 648 °C, but no intermediate mode is seen as shown in Fig. 4(b). Hence these modes most likely do not arise from a N-pair defect and cannot be related to the pair modes observed at 402 °C. Apparently a new mode appears around 450 °C; this mode coincides with the 659-cm^{-1} pair mode observed in ^{14}N-implanted samples and is only shifted by 3 cm^{-1} from the 640-cm^{-1} pair mode seen in ^{15}N-implanted samples. This mode, marked by a * in Table I, causes the shoulder on the annealing curve of the 659-cm^{-1} mode shown in Fig. 4(a) above 600 °C. Based on this it is our firm belief that the 659- and 825-cm^{-1} pair modes do disappear together, and hence that the pair modes arise from the same N-pair defect.

Finally, we may also conclude that the two N atoms of the pair must be equivalent as only two intermediate modes (654 and 810 cm^{-1}) are observed in the sample implanted with both ^{14}N and ^{15}N. If the N atoms were inequivalent then four intermediate modes should have appeared.

The frequencies and widths of the N pair modes in Ge are in Table II compared to those of the N pair modes in Si. Contrary to Si, Ge has several isotopes of comparable abundances but the width of the N pair modes in Ge is not determined by this as no splitting of the individual modes could be resolved by increasing the resolution. Moreover, the modes are sharper in Ge than in Si. This is most likely due to the larger mass of the Ge atoms which makes the N modes more localized in Ge than in Si and due to the fact that the pair modes may decay by two-phonon processes in Si but only by three-phonon or higher-order processes in Ge. As shown in Fig. 2 the widths of the ^{15}N pair modes are much broader than those of the ^{14}N modes in Ge. This was also observed by Stein[8] and is not seen for the N pair modes in Si. Stein suggested that this reflected different levels of disorder created by the different isotopes in the implanted layer. We do not consider that this explanation is correct as the width of the 825-cm^{-1} mode is the same in the pure ^{14}N sample as in the mixed isotopic sample (see Fig. 2). Since the phonon spectrum of Ge does not show any particularly strong features at the positions of the ^{15}N modes the difference in widths is unlikely to be caused by simple phonon interaction. Further work is needed to understand these linewidths.

TABLE II. Local vibrational pair modes observed in Ge after anneal at 402 °C and in Si after anneal at 650 °C. The stated width is the full width at half maximum as determined from spectra with 1 cm^{-1} resolution.

Isotope	^{14}N	^{15}N	$^{14,15}N$, intermediate modes
Ge: (77 K)			
Position (cm^{-1})	825.3 658.6	799.4 640.0	809.7 653.7
Width (cm^{-1})	4.1 3.0	7.6 6.3	4.1 7.5
Si: (300 K)			
Position (cm^{-1})	962.6 765.9	936.3 748.5	947.2 758.7
Width (cm^{-1})	9.6 8.0	8.7 6.9	8.2 7.0

A calibration coefficient relating the absorption of the N pair modes to the concentration of N in such pairs has been determined for N in Si.[11] Using this relation it was found[7] that the N pairs are by far the most abundant N defect in Si. To the best of our knowledge a corresponding calibration factor does not exist in the case of N in Ge. However, the N pair is the most prominent N-related defect observed by infrared absorption in Ge and the only one observed just after recrystallization (flow oven anneal). This is analogous to N in Si and strongly suggests that the N pair is also the dominant N defect in Ge.

In his work Stein[8] also observed a mode at 577 cm^{-1} assigned to substitutional N and a mode at 590 cm^{-1} ascribed to an N interstitial. These two modes were not observed in this work but this is not unexpected. It is well known[10] that detectable amounts of substitutional N in Si can only be achieved by ion implantation followed by laser annealing. If this is also true for Ge we would not expect to observe substitutional N in oven-annealed samples. Furthermore, although we observed[12] a mode at 691 cm^{-1} for N-implanted Si followed by a single anneal at 600 °C in a flow oven, this was not observed in an annealing experiment of the type described here. We consider that substitutional and interstitial N defects are mobile during annealing and that rapid recrystallization and cooling are necessary to trap N as N_s or N_i in both Si and Ge. This explains why we do not observe the 577- and 590-cm^{-1} modes.

V. THEORETICAL CALCULATIONS

We now describe the results of local-density-functional calculations carried out on Ge containing N defects using norm-conserving pseudopotentials[13] and large hydrogen-(H) terminated clusters. The wave functions of the clusters are expanded in *s*- and *p*-type Gaussians and the charge density is fitted to *s*-type Gaussians situated at atomic nuclei and the centers of bonds. We used eight Gaussian orbitals with different exponents at each Ge and N site and two at each of the terminating H nuclei. The charge density was fitted with eight Gaussian functions at both Ge and N sites and three at the H ones. In addition, a Gaussian orbital and fitting function were situated at each bond center. The self-consistent energy was found for each structure along with the analytic forces on each atom. The cluster was then relaxed using a conjugate gradient method. More details of the method have been given previously.[14] First we studied a 71-atom

cluster, $Ge_{35}H_{36}$, representing pure Ge and containing four shells of Ge atoms surrounding a central one. All Ge atoms were allowed to relax and we found that the Ge-Ge bond length between the innermost atoms was 2.41 Å. This is within 1.6% of the experimental value of 2.45 Å. The energy double derivatives between the five inner atoms were then calculated and fitted to those of a Musgrave-Pople potential where the potential for atom i is

$$V_i=\tfrac{1}{4}\sum_j k_r^{(i)}(\Delta r_{ij})^2+\frac{r_0^2}{2}\sum_{j>k} k_\theta^{(i)}(\Delta\theta_{jik})^2 + r_0\sum_{k>j} k_{r\theta}^{(i)}(\Delta r_{ij}+\Delta r_{ik})\Delta\theta_{jik} + \sum_{k>j} k_{rr}^{(i)}\Delta r_{ij}\Delta r_{ik}+r_0^2\sum_{l>k>j} k_{\theta\theta}^{(i)}\Delta\theta_{jik}\Delta\theta_{kil}\ .$$

Here Δr_{ij} and $\Delta\theta_{jik}$ are the changes in the length of the i-j bond and the angle between the i-j and i-k bond, respectively. The sum is over the nearest-neighbor atoms only. Table III gives the coefficients $k_r^{(i)}$, $k_\theta^{(i)}$, $k_{r\theta}^{(i)}$, $k_{rr}^{(i)}$, and $k_{\theta\theta}^{(i)}$. This potential can then be used to derive the phonon spectrum for the bulk solid.

The Raman frequency found in this way lies at 300 cm^{-1} (^{74}Ge) which is to be compared with the experimental one at 304 cm^{-1}. The calculated phonon frequencies at other high-symmetry points of the Brillouin zone are given in Table IV compared to the values obtained by neutron scattering.[15] In general the agreement between calculated and observed values is good except for the transverse acoustic (TA) mode near the X point. The observed flattening of the TA phonon curve at the X point is a well-known long-range effect which is not described by a short-range potential.

We then considered the substitutional N defect. For this calculation the central Ge atom of the 71-atom cluster was replaced by N and the cluster rerelaxed. The N atom moved off site along ⟨111⟩ so that one N-Ge bond became extremely long at 3.58 Å and the three others became 1.96 Å. The displacement of the N atom from the lattice site is 0.63 Å. This is similar to the ⟨111⟩ distortion calculated previously for N in Ge, Si, and diamond.[7,16–20]

There is a single gap level close to the conduction band. The vibrational modes were found from the double derivatives between the five inner atoms and the remaining entries in the dynamical matrix given by the Musgrave-Pople potential above. The highest mode is a doublet occurring at 574.4 cm^{-1} (^{74}Ge) and is in good agreement with that assigned to substitutional N at 577 cm^{-1} by Stein. The mode shifts to 572.2 cm^{-1} with ^{72}Ge.

We then looked at the Si-N split interstitial. For this an N atom was added to the original 71-atom cluster which was then relaxed. We found the resulting defect possesses C_{2v} symmetry (⟨100⟩ orientation) with the three N-Ge bonds being almost equal at 1.90, 1.91, and 1.91 Å and the Ge atom with the dangling bond having Ge bonds of lengths 2.304 Å. The vibrational modes were worked out from the double derivatives of the inner six atoms and are given in Table V. The two highest modes at 648.4 and 617.1 cm^{-1} are rather close together, but only one, assigned by Stein to this defect, has been reported at 590 cm^{-1}. The modes shift to 649.0 and 617.7 cm^{-1} for ^{72}Ge. The higher mode corresponds to the stretch of the two N-Ge bonds along ⟨011⟩ and the lower to a ⟨100⟩ N-Ge stretch.

Finally, the structure and LVM's of the pair of closeby ⟨100⟩ split interstitials shown in Fig. 1 were investigated using a large 88-atom cluster, $N_2Ge_{35}H_{36}$, centered on the middle of a bond. Again all atoms were relaxed and the defect was found to be stable with Ge-N bond lengths of $a=1.83$ and $b=1.88$ Å and an internal bond angle $\Theta=93°$ (see Fig. 1). The defect retained C_{2h} symmetry as found for the same defect in Si.[7] The contributions to the dynamical matrix from the two N atoms and the two Ge atoms forming the square as well as the surrounding six Ge atoms were calculated directly. The other Ge-Ge contributions were found from the Musgrave-Pople potential mentioned above.

As appropriate for a pair defect the antiparallel model of Fig. 1 gives rise to six N-related modes. However, two of these fall below the Raman frequency and such modes are broadened significantly and hence hardly observed.[21] The calculated frequencies of the four modes above the Raman frequency (^{74}Ge cluster) are shown together with the observed modes in Table V. The C_{2h} symmetry of the defect makes the two nondegenerate modes labeled B_u infrared active at 754 and 632 cm^{-1} and these are to be compared with the observed modes at 825 and 659 cm^{-1}. Thus our deviations are less than 72 cm^{-1} and are typical for the method.[7] For the high-frequency mode all the calculated isotopic shifts agree with the measured ones within 2.5 cm^{-1}. For the low-frequency mode the calculated isotopic shift in replacing ^{14}N with ^{15}N deviates by 1.7 cm^{-1} from the measured shift, whereas the errors in the calculated mixed isotopic shifts in this case are larger but within the uncertainty of the method.

The natural abundance of ^{74}Ge is 36.7% while, e.g., the abundance of ^{72}Ge is 27.4%. If ^{74}Ge is substituted by ^{72}Ge in the cluster the high-frequency mode at 753.8 cm^{-1} shifts by 0.83 to 754.6 cm^{-1}. The low-frequency

TABLE III. Musgrave-Pople potential for Ge in eV/Å^2, $r_0=2.348$ Å.

k_r	k_θ	$k_{r\theta}$	k_{rr}	$k_{\theta\theta}$
7.661	0.323	−0.075	0.911	0.105

TABLE IV. Calculated and observed (Ref. 15) phonon frequencies (cm^{-1}) in Ge for some high-symmetry points in the first Brillouin zone.

Γ calculated	300			
Γ observed	304			
	TA	LA	TO	LO
L calculated	76	227	272	242
L observed	63	222	290	245
X calculated	119	240	253	246
X observed	80	241	276	241

TABLE V. Calculated (^{74}Ge) and observed local vibrational modes in cm^{-1} of N defects in Ge.

Substitutional N							
Calculated		574.4					
Observed		577					
Interstitial N							
Calculated		648.4		617.1			
Observed		590					
N pair							
Calculated					Observed (77 K, this work)		
^{14}N	^{15}N	^{14,15}N	IR active	Mode	^{14}N	^{15}N	^{14,15}N
632.1	611.8	620.6	yes	B_u	658.6	640.0	653.7
711.2	688.3	700.5	no	A_g			
753.8	730.3	739.1	yes	B_u	825.3	799.4	809.7
789.7	763.8	780.3	no	A_g			

mode shifts by 0.47 from 632.1 to 632.5 cm^{-1}. These shifts are both much smaller than the observed widths of the LVM's (see Table II) and explain why we do not observe any splitting due to the different isotopes of Ge.

VI. DISCUSSION

Cunha, Canuto, and Fazzio have recently[16] suggested that N pairs should be formed by pairing on adjacent lattice sites in all group-IV semiconductors. In this model the two N atoms distort from the lattice sites in opposite ⟨111⟩ directions leading to no or very weak bonding between the N atoms. Although there is evidence that this is the stable defect in diamond,[19,20,22] we do not favor this model of the N pair in either Si or Ge as discussed recently.[23] This is because (a) the N-N interaction is expected to be too low to account for the occurrence of intermediate modes in samples containing both ^{14}N and ^{15}N, (b) the suggested ⟨111⟩ displacement of the N atoms in Si is inconsistent with channeling measurements on N-implanted Si,[5,24] and (c) in both Si and Ge, the LVM's arising from a ⟨111⟩-oriented pair should be rather close to the one of substitutional N and well below those actually observed.

In Si the antiparallel "squarelike" configuration shown in Fig. 1 was suggested[7] as a model of the N pair and, as shown in this paper, the same configuration is fully consistent with the observed infrared absorption of the N pair in Ge. The antiparallel model is attractive as all Ge atoms are tetravalently bonded and both N atoms have three Ge-N bonds with bond lengths closely resembling those found in molecular compounds such as trigermylamine, $(GeH_3)_3N$. This compound has an almost planar structure, it shows a broad absorption band at 850 cm^{-1} ascribed to a Ge-N stretch mode, and has Ge-N bond lengths of 1.836 Å.[25,26]

The observed agreement between the infrared absorption and the calculation together with the fact that the same model accounts for all the properties of the N-pair defect in Si lends strong support to the antiparallel model for the N pair in Ge. The pair defect is the most prominent N-related defect observed with infrared absorption and it is electrically inert. The low solubility of N in Ge and the tendency for N to form inactive pairs ensures that the doping efficiency of N in Ge is low. The substitutional N defect has been found theoretically to distort along ⟨111⟩—as found previously for N_s in Ge, Si, and diamond. The ⟨100⟩ Ge-N split interstitial is also stable. The calculated modes of these two defects lie close to those found by Stein and support his assignments.

VII. CONCLUSIONS

This study has concentrated on two N-related local vibrational modes in Ge previously observed by Stein. Through measurement of the infrared absorption on samples implanted with different isotopes of N and via annealing studies, it has been shown that these modes arise from the same defect involving a pair of equivalent N atoms. Based on this and *ab initio* theory we propose the model shown in Fig. 1 of the N pair in Ge. The fact that the N pair in Si was found to have the same structure as the one proposed here in Ge strongly supports this model of the pair defect. Furthermore, the model offers an explanation to the low donor efficiency of N in Ge.

The C_i-O_i pair in Si was recently found[27] to have a squarelike structure similar to the one determined here for the N pair, and such a configuration has also been suggested[28] as a low-energy saddle point for the migration of the O dimer also in Si. The square structure is therefore possibly a basic one for various pairs of impurities in Si and Ge.

ACKNOWLEDGMENTS

We gratefully acknowledge B. Bech Nielsen for his continuing interest in this project and for several fruitful discussions. This project has been supported by the Danish Natural Research Council, jr. nr. 11-7961 and the Danish National Research Foundation through the Aarhus Center for Advanced Physics (ACAP).

[1]P. V. Pavlov, E. I. Zorin, D. I. Tetelbaum, and A. F. Khoklov, Phys. Status Solidi A **35**, 11 (1976).
[2]A. B. Campbell, J. B. Mitchell, J. Shewchun, D. A. Thompson, and J. A. Davies, Can. J. Phys. **53**, 303 (1975).
[3]Y. Yatsurugi, N. Akiyama, Y. Endo, and T. Nozaki, J. Electrochem. Soc. **120**, 975 (1973).
[4]J.-H. Zhou, K. Yamaguchi, Y. Yamamoto, and T. Shimizu, J. Appl. Phys. **74**, 5086 (1993).
[5]I. Chambouleyron and A. R. Zanatta, Appl. Phys. Lett. **62**, 58 (1993).
[6]H. J. Stein, in *Oxygen, Carbon, Hydrogen, and Nitrogen in Crystalline Silicon,* edited by J. C. Mikkelsen, Jr., S. J. Pearton, J. W. Corbett, and S. J. Pennycook, MRS Symposia Proceedings No. 59 (Materials Research Society, Pittsburgh, 1986), p. 523.
[7]R. Jones, S. Öberg, F. Berg Rasmussen, and B. Bech Nielsen, Phys. Rev. Lett. **72**, 1882 (1994).
[8]H. J. Stein, Appl. Phys. Lett. **52**, 153 (1988).
[9]K. L. Brower, Phys. Rev. B **26**, 6040 (1982).
[10]H. J. Stein, Appl. Phys. Lett. **47**, 1339 (1985).
[11]Y. Itoh, T. Nozaki, T. Masui, and T. Abe, Appl. Phys. Lett. **47**, 488 (1985).
[12]F. Berg Rasmussen and B. Bech Nielsen (unpublished).
[13]G. B. Bachelet, D. R. Hamann, and M. Schlüter, Phys. Rev. B **26**, 4199 (1982).
[14]R. Jones, Philos. Trans. R. Soc. London Ser. A **341**, 351 (1992).
[15]G. Nilsson and G. Nelin, Phys. Rev. B **3**, 364 (1971).
[16]C. Cunha, S. Canuto, and A. Fazzio, Phys. Rev. B **48**, 17 806 (1993).
[17]G. G. DeLeo, W. B. Fowler, and G. D. Watkins, Phys. Rev. B **29**, 3193 (1984).
[18]H. P. Hjalmarson and D. R. Jennison, Phys. Rev. B **31**, 1208 (1985).
[19]P. R. Briddon, R. Jones, and M. I. Heggie, in *International Conference on New Diamond Science and Technology,* edited by R. Messier, J. T. Glass, J. E. Butler, and R. Roy, MRS Symposia Proceedings No. 63 (Materials Research Society, Pittsburgh, 1991).
[20]R. Jones, P. R. Briddon, and S. Öberg, Philos. Mag. Lett. **66**, 67 (1992).
[21]R. C. Newman, *Infra-red Studies of Crystal Defects* (Taylor & Francis, London, 1973).
[22]G. Davies, J. Phys. C **9**, L537 (1976).
[23]F. Berg Rasmussen, B. Bech Nielsen, R. Jones, and S. Öberg (unpublished).
[24]F. Berg Rasmussen and B. Bech Nielsen, Phys. Rev. B **49**, 16 353 (1994).
[25]C. Glidewell, D. W. H. Rankin, and A. G. Robiette, J. Chem. Soc. A **(1970)** 2935.
[26]D. W. H. Rankin, J. Chem. Soc. A **(1969)** 1926.
[27]R. Jones and S. Öberg, Phys. Rev. Lett. **68**, 86 (1992).
[28]P. Deak, L. C. Snyder, and J. W. Corbett, Phys. Rev. B **45**, 11 612 (1992).

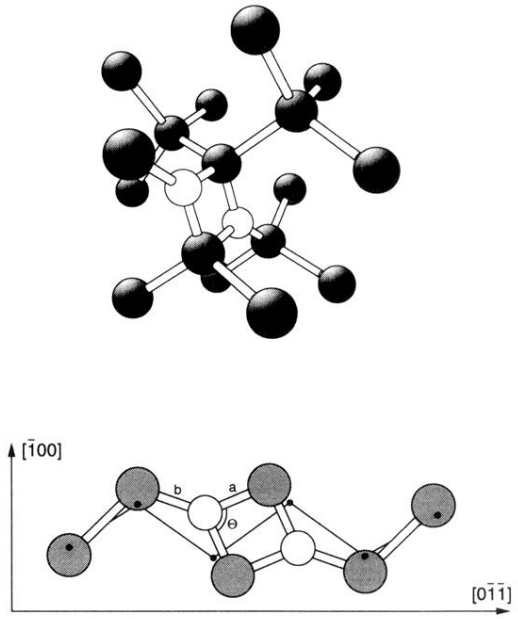

FIG. 1. The antiparallel model of the N pair defect (Ref. 7) shown in perspective and in the {110} mirror plane. The small points mark the substitutional (perfect lattice) sites. The upper part of the figure has been reproduced from Ref. 7.